

Received 20xx month day; accepted 20xx month day

## Galaxy interactions in filaments and sheets: insights from EAGLE simulations

Apashanka Das<sup>1</sup>, Biswajit Pandey<sup>2</sup> and Suman Sarkar<sup>3,4</sup>

<sup>1</sup> Department of Physics, Visva-Bharati University, Santiniketan, Birbhum, 731235, India  
[a.das.cosmo@gmail.com](mailto:a.das.cosmo@gmail.com)

<sup>2</sup> Department of Physics, Visva-Bharati University, Santiniketan, Birbhum, 731235, India  
[biswap@visva-bharati.ac.in](mailto:biswap@visva-bharati.ac.in)

<sup>3</sup> Department of Physics, Indian Institute of Science Education and Research Tirupati, Tirupati - 517507, India

<sup>4</sup> Department of Physics, Indian Institute of Technology Kharagpur, Kharagpur, 721302, India  
[suman2reach@gmail.com](mailto:suman2reach@gmail.com)

**Abstract** We study the colour and star formation rates of paired galaxies in filaments and sheets using the EAGLE simulations. We find that the major pairs with pair separation  $< 50$  kpc are bluer and more star forming in filamentary environments compared to those hosted in sheet-like environments. This trend reverses beyond a pair separation of  $\sim 50$  kpc. The interacting pairs with larger separations ( $> 50$  kpc) in filaments are on average redder and low-star forming compared to those embedded in sheets. The galaxies in filaments and sheets may have different stellar mass and cold gas mass distributions. Using a KS test, we find that for paired galaxies with pair separation  $< 50$  kpc, there are no significant differences in these properties in sheets and filaments. The filaments transport gas towards the cluster of galaxies. Some earlier studies find preferential alignment of galaxy pairs with filament axis. Such alignment of galaxy pairs may lead to different gas accretion efficiency in galaxies residing in filaments and sheets. We propose that the enhancement of star formation rate at smaller pair separation in filaments is caused by the alignment of galaxy pairs. A recent study with the SDSS data (Das, Pandey & Sarkar 2023) reports the same findings. The confirmation of these results by the EAGLE simulations suggests that the hydrodynamical simulations are powerful theoretical tools for studying the galaxy formation and evolution in the cosmic web.

**Key words:** methods: data analysis — statistical — galaxies: interactions — evolution — cosmology: large scale structure of the universe

### 1 INTRODUCTION

The galaxies are the fundamental units of the observed large-scale structures in the Universe. Understanding their formation and evolution is one of the primary goals of modern cosmology. The growth of the primordial density perturbations via the gravitational instability eventually leads to the formation of the dark matter halos. The dark matter halos represent the peaks in the density field. The halos are surrounded by diffuse neutral Hydrogen distribution after the recombination. They accrete the

gas which radiate away their kinetic energy and settle down at their centers. The cooling and condensation of the gas at the centre of these halos are believed to be the primary mechanism for galaxy formation (Silk 1977; White & Rees 1978).

The formation and evolution of galaxies are expected to be influenced by both the initial conditions at the location of their formation and their interactions with the surrounding environment. The galaxies interact with other galaxies in their neighbourhood. The galaxy-galaxy interactions are known to amplify the star formation rate in galaxies (Barton, Geller & Kenyon 2000; Nikolic, Cullen & Alexander 2004; Woods & Geller 2007; Ellison et al. 2010; Patton et al. 2011). The environments of galaxies have crucial roles in their evolution. The colour and star formation rates of galaxies are strongly affected by the local density of their environment (Gómez et al. 2003; Lewis et al. 2002). The galaxies become redder and low-star forming in the higher density environments (Kauffmann et al. 2004). The suppression of star formation can be driven by different physical mechanisms. The ram pressure stripping is a common phenomena in galaxy clusters (Gunn & Gott 1972). The galaxies in the high density regions are more likely to encounter harassment (Moore et al. 1996; Moore, Lake & Katz 1998), starvation (Larson, Tinsley & Caldwell 1980; Somerville & Primack 1999), strangulation (Gunn & Gott 1972; Balogh, Navarro & Morris 2000) and gas expulsion by supernovae, AGN or stellar winds (Cox et al. 2004; Murray, Quataert & Thompson 2005; Springel, Matteo & Hernquist 2005). The star formation in galaxy may also quench through several other routes. The mass (Birnboim & Dekel 2003; Dekel & Birnboim 2006), morphology (Martig et al. 2009), presence of bar (Masters et al. 2010) and high angular momentum (Peng & Renzini 2020) can cease the star formation activity in galaxies.

Many other galaxy properties depend on the environment. The elliptical galaxies are more commonly observed in dense groups and clusters (Oemler 1974; Dressler 1980; Davis & Geller 1976; Guzzo et al. 1997; Goto et al. 2003). The spiral galaxies mostly occupy the intermediate and low density regions of the Universe. These environmental dependencies of clustering are reflected in different statistical measures such as the correlation function (Zehavi et al. 2005), genus (Park et al. 2005), filamentarity (Pandey & Bharadwaj 2005, 2006), local dimension (Pandey & Sarkar 2020) and mutual information (Pandey & Sarkar 2017; Bhattacharjee, Pandey & Sarkar 2020; Sarkar & Pandey 2020). The environment of a galaxy is generally characterized by the local density. The local density undoubtedly plays a decisive role in galaxy evolution. However, it can not completely characterize the environment of a galaxy. The early generation redshift surveys reveal that galaxies are part of an all-inclusive network comprising clusters, filaments and sheets surrounded by vast empty regions (Joeveer & Einasto 1978; Gregory & Thompson 1978; Einasto, Joeveer, & Saar 1980; Zeldovich & Shandarin 1982). The galaxies and their host halos are embedded in different environments of the cosmic web (Bond, Kofman & Pogosyan 1996). Pandey & Bharadwaj (2008) find that the star forming blue galaxies trace a more filamentary distribution compared to the red galaxies. More than 80% of the baryonic budget in the Universe is accounted by low density gas (WHIM) in filaments (Tuominen 2021; Galarraga-Espinosa et al. 2021). Consequently, the gas accretion efficiency of the dark matter halos in different environments may differ in a significant manner. Thus, the cosmic web can have significant impact on the galaxy properties and their evolution. The galaxies that are located in different parts of the cosmic web can experience different physical conditions, such as different densities of gas, different levels of tidal forces, different frequency of interactions and mergers.

The interactions between galaxies with comparable masses are known as the major interactions. Such interactions trigger new star formation in galaxies. The interacting pairs can be hosted in different morphological environments of the cosmic web. The galaxy pairs are more frequently observed in the denser regions. The filaments and sheets, being the denser parts of the cosmic web, can host a significant number of major galaxy pairs. In a recent work, Das, Pandey & Sarkar (2023) analyze the SDSS data to compare the star formation rate and colour of major pairs hosted in filaments and sheets. They find that the major galaxy pairs with separation  $< 50$  kpc are relatively high star forming and bluer when hosted in filaments. Contrarily, the major pairs at separations larger than 50 kpc show a significantly higher SFR and bluer colour in sheet-like environments. This behaviour may be related to the preferential alignment of galaxy pairs with the filament axis reported in a number of recent works (Tempel & Tamm 2015; Mesa et al. 2018). The star formation in a galaxy is primarily regulated by its available gas mass.

The inflows and outflows (Dekel, Sari, & Coverino 2009; Davé, Finlator, & Oppenheimer 2012) can significantly modulate the gas mass in a galaxy. The transient events like interactions and mergers can drive the galaxies out of equilibrium. The alignment of galaxy pairs with filament spines may lead to anisotropic accretion and higher gas accretion efficiency in these galaxies. In this work, we intend to verify these findings using hydrodynamical simulations.

The EAGLE simulation (McAlpine et al. 2016) is a hydrodynamical simulation that studies the galaxy formation and evolution in a cosmological volume. It describes the formation of galaxies by gas falling into the dark matter halos and their subsequent cooling and condensation. It would be interesting to study the colour and star formation rate in the major pairs in filaments and sheets using EAGLE simulations. In observations, the galaxy pairs are usually identified by applying simultaneous cuts on the projected separation and the velocity difference of the galaxies in the rest frame. However, all these pairs may not be undergoing interactions. Some of the pairs identified in observations may not be close in three dimensions due to the chance superposition in the high-density regions like groups and clusters (Alonso et al. 2004). Also, we can not construct a mock catalogue for the observational sample of galaxy pairs used in Das, Pandey & Sarkar (2023) due to the smaller volume of the EAGLE simulations. So we decided to use the real-space positions of galaxies available in simulation to identify the major pairs. This would avoid any errors in identification of galaxy pairs due to the projection effects. We identify the geometric environments of galaxy pairs using the local dimension (Sarkar & Bharadwaj 2009). Our primary aim of this work is to study the interaction induced star formation in filaments and sheets using EAGLE simulations. This would help us to assess the roles of the filaments and sheets in galaxy evolution.

We organise the structure of the paper as follows: we describe the data and the method of analysis in Section 2 and present the results and conclusions in Section 3.

## 2 DATA AND METHOD OF ANALYSIS

### 2.1 EAGLE simulation data

The EAGLE simulation (McAlpine et al. 2016) is a set of cosmological hydrodynamical simulation in periodic, cubic comoving volumes ranging from side of length 25 to 100 Mpc. It tracks the evolution of both baryons and dark matter in the Universe from a redshift of 127 to 0. The simulation adopts a flat  $\Lambda$ CDM cosmology with  $\Omega_\Lambda = 0.693$ ,  $\Omega_m = 0.307$ ,  $\Omega_b = 0.04825$  and  $H_0 = 67.77$  km/s/Mpc (Planck Collaboration et al. 2014).

We download the various properties of galaxies from the publicly available EAGLE run simulation. We extract the information of position of the centre of mass of galaxies in three dimensions within a comoving cubic volume of size  $100 \text{ Mpc}^3$  from *Ref-L0100N1504\_Subhalo* table. We consider the last snapshot of the simulation having *Snapnum* = 28 which corresponds to redshift  $z = 0$ . We select only those galaxies which are flagged as *Spurious* = 0. This ensures that we select only the genuine simulated galaxies by discarding all the unusual objects with anomalous stellar mass, metallicity or black hole mass. We also download the star formation rate, stellar mass and cold gas mass of simulated galaxies using *Ref-L0100N1504\_Aperture* table. These are estimated within a spherical 3D aperture of radius 30 kpc centered at the location of the minimum gravitational potential of a galaxy. Use of this criteria gives well suited stellar mass and star formation estimates as compared to observational results and is also recommended for use by the EAGLE simulation team (McAlpine et al. 2016). We also consider only those galaxies with a stellar mass  $> 0$ . Combining the two tables with *GalaxyID*, we obtain all of the above mentioned information for 325358 galaxies. We also extract the rest frame broadband magnitudes of galaxies estimated in *u* and *r* band filters (Doi et al. 2010) from *Ref-L0100N1504\_Magnitude* table, where *u* and *r* respectively denote Ultraviolet and Red filter bands of Sloan Digital Sky Survey (SDSS). We combine this table with *Ref-L0100N1504\_Subhalo* and *Ref-L0100N1504\_Aperture* table using *GalaxyID* to get all the required information. The magnitude of galaxies in different SDSS filters are also computed in 30 kpc spherical apertures (Trayford et al. 2015). Finally, we have all these information for 29754 galaxies. For the rest of the analysis, we refer to *u-r*

Morphological environment	Local dimension
$D1$	$0.75 \leq D < 1.25$
$D2$	$1.75 \leq D < 2.25$
$D3$	$D \geq 2.75$
$D1.5$	$1.25 \leq D < 1.75$
$D2.5$	$2.25 \leq D < 2.75$

Table 1: This table shows the definition of different geometric environments based on the local dimension ( $D$ ) of the galaxies.

colour of galaxies as the difference of its rest frame non-dust attenuated absolute magnitudes in  $u$  and  $r$  band respectively. Only the magnitudes of the galaxies with stellar mass  $\log(M_{\text{stellar}}/M_{\text{sun}}) > 8.5$  are provided in *Ref - L0100N1504\_Subhalo* table. However, here we use the stellar mass estimates of galaxies from *Ref - L0100N1504\_Aperture* table where the minimum stellar mass of a galaxy is  $\log(M_{\text{stellar}}/M_{\text{sun}}) \sim 8.2$ . Observations show that the galaxies with stellar mass  $M_{\text{stellar}} < 3 \times 10^{10} M_{\text{sun}}$  are actively star forming and the galaxies having stellar masses above this critical value are generally quiescent systems (Kauffmann et al. 2003). For the present analysis, we consider only those galaxies which have their stellar mass in between  $8.5 \leq \log(M_{\text{stellar}}/M_{\text{sun}}) \leq 10.5$ . Our mass limited sample contains a total 21305 galaxies.

We identify the nearest neighbour in three dimensions for each galaxy in our mass limited sample. We denote the distance to the nearest neighbour for each galaxy by  $r$ . Here distance refers to the 3D physical separation between the centre of mass of the galaxies. Initially, we label each galaxy and its nearest neighbour in our sample as a possible pair. We then select only those pairs for which  $r \leq 200$  kpc. We also apply a cut on their stellar mass ratio  $1 \leq \frac{M_1}{M_2} < 3$  to include only the major pairs in our analysis. This provides us with a total 2264 major pairs. The smallest pair separation in our sample is  $\sim 6$  kpc.

We determine the morphological environment of the galaxies in the EAGLE simulation by estimating their local dimension (subsection 2.2). We use *GalaxyID* to cross match these galaxies with our pair sample. The cross-matching yields a total 2537 galaxies in major pairs. We find that 373 and 276 out of these galaxies are residing in filaments and sheets respectively. It may be noted that we can not determine the local dimension of all the galaxies in the simulation.

## 2.2 Geometry of the local environment

We characterize the different geometric environments of the cosmic web using the local dimension (Sarkar & Bharadwaj 2009). The local dimension is a simple measure based on the galaxy counts within spheres of different radii centered on a galaxy. The galaxy counts within a sphere of radius  $R$  centered on a galaxy can be written as,

$$N(< R) = A R^D \quad (1)$$

where  $D$  is the local dimension and  $A$  is an arbitrary constant. The number counts  $N(< R)$  would scale differently with the radius  $R$  depending on the local geometry of the embedding environment. The radius of the sphere around each galaxy is varied between  $R_1 \text{ Mpc} \leq R \leq R_2 \text{ Mpc}$  and the galaxy counts are measured for each radius. Only the galaxies that have at least 10 neighbouring galaxies within this range are considered for this analysis. We fit the observed number counts  $N(< R)$  to Equation 1 using a least-square fitting. The goodness of each fit is determined by estimating the  $\chi^2$  per degree of freedom. We only retain the fits having  $\frac{\chi^2}{\nu} \leq 0.5$  (Sarkar & Pandey 2019) and discard the rest from our analysis. We choose  $R_1 = 2 \text{ Mpc}$  and  $R_2 = 10 \text{ Mpc}$  for the analysis presented here.

The local dimension  $D$  describes the morphology of the embedding environment. Ideally, a filamentary environment should have  $D = 1$  and sheet-like environment should have  $D = 2$ . A homogeneous distribution in three-dimension is represented by  $D = 3$ . However, the filaments, sheets, clusters and voids are not idealized structures and they can have a wide variety of shapes and sizes. Each geometric environment is assigned a range of local dimension Table 1. A nearly straight filament is represented

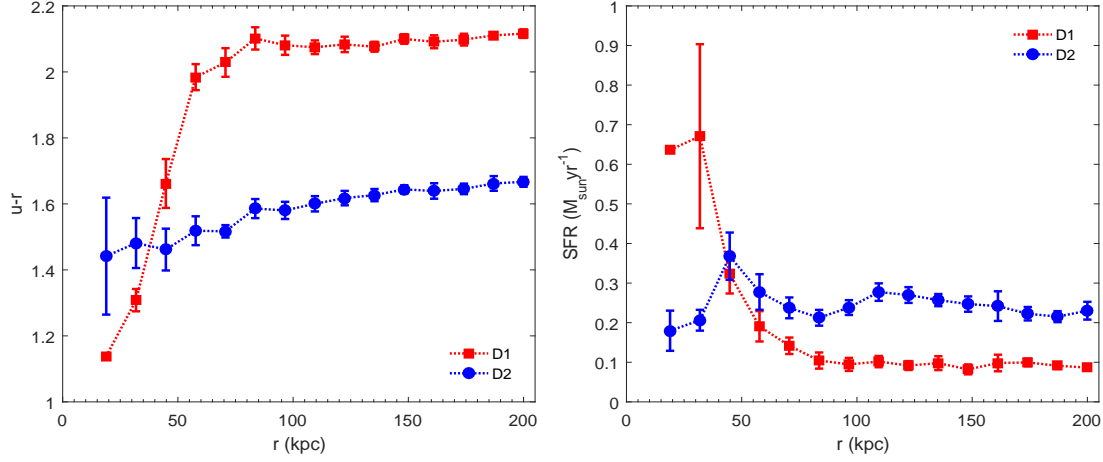


Fig. 1: The left panel of this figure shows the cumulative mean  $u-r$  colour as a function of pair separation for major pairs residing in  $D1$  and  $D2$  type environments. The right panel shows the cumulative mean SFR for the same pairs in two different environments. We use 10 Jackknife samples to estimate the  $1\sigma$  error bars shown at each data point.

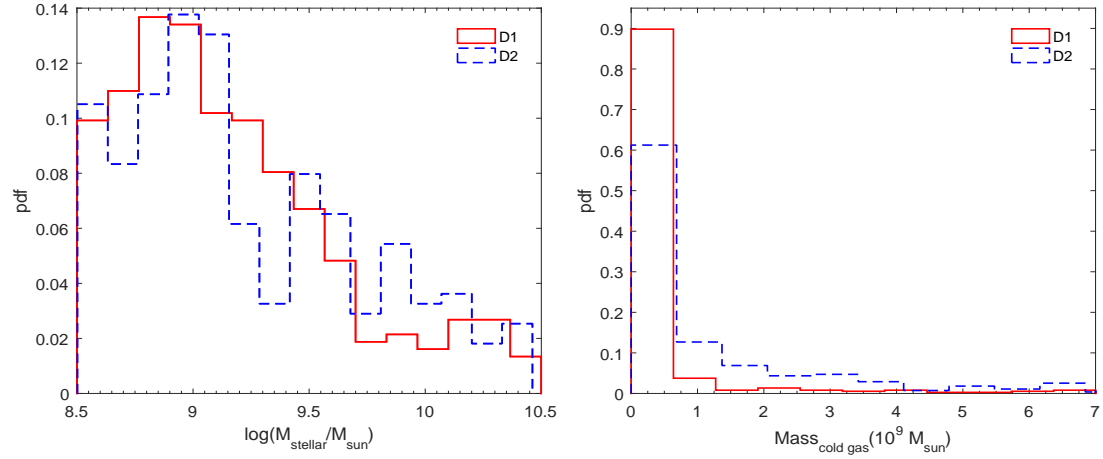


Fig. 2: The left panel shows the probability distribution function of  $\log(M_{\text{stellar}}/M_{\text{sun}})$  for major pairs in  $D1$  and  $D2$  type environments. The right panel shows the probability distribution function of  $\text{Mass}_{\text{cold gas}}$  for the same pairs.

by  $D1$ -type environment. Similarly, the  $D2$ -type environment represents a two-dimensional sheet-like structure. A  $D3$ -type environment is embedded in a three dimensional distribution of homogeneous nature. The galaxies can also reside near the junction of different types of morphological environments.  $D1.5$  and  $D2.5$  can be treated as intermediate environments.

### 3 RESULTS AND CONCLUSIONS

The cumulative mean of the  $u-r$  colour for the major galaxy pairs as a function of the pairs separation is shown in the left panel of Figure 1. We compare the results for the major pairs in filaments and sheets in the same panel.

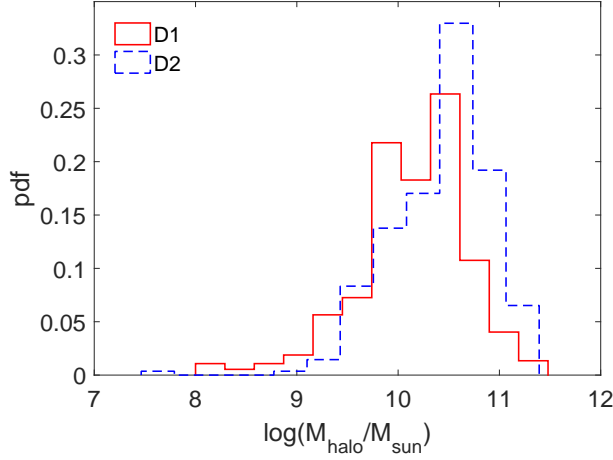


Fig. 3: This figure shows the distributions of the halo mass of paired galaxies in sheets and filaments.

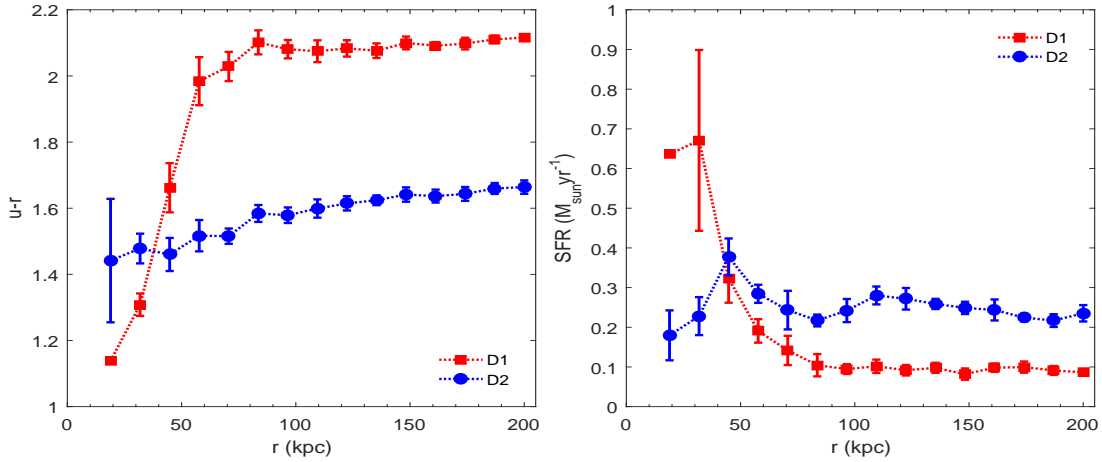


Fig. 4: Same as Figure 1 but when the galaxy positions are defined by the location of the minimum of the gravitational potential instead of the centre of mass.

This shows that the major pairs with pair separation  $r < 50$  kpc are on average bluer in filamentary environment compared to those residing in sheet-like environment. However, this trend only persists up to a pair separation of  $\sim 50$  kpc. A cross over of the two curves corresponding to  $D1$  and  $D2$  type environments is observed at  $r \sim 50$  kpc. The major pairs with pair separation  $r > 50$  kpc are significantly redder in filaments compared to those located in sheets. We also analyze the SFR in major pairs residing in filaments and sheets and show the results in the right panel of Figure 1. We find that the major pairs at closer pair separation ( $< 50$  kpc) in filaments are comparatively more star forming than those located in sheets. We see an exactly opposite trend for the major pairs with larger pair separation ( $> 50$  kpc). The colour of the galaxies are strongly correlated with their SFR (Baldry et al. 2004) and the results shown in the two panels of Figure 1 are consistent with each other. It is also interesting that the crossover is observed at nearly the same pair separation ( $\sim 50$  kpc) for both colour and SFR. We estimate the  $1-\sigma$  error bars at each pair separation using 10 Jackknife samples drawn from the original datasets.

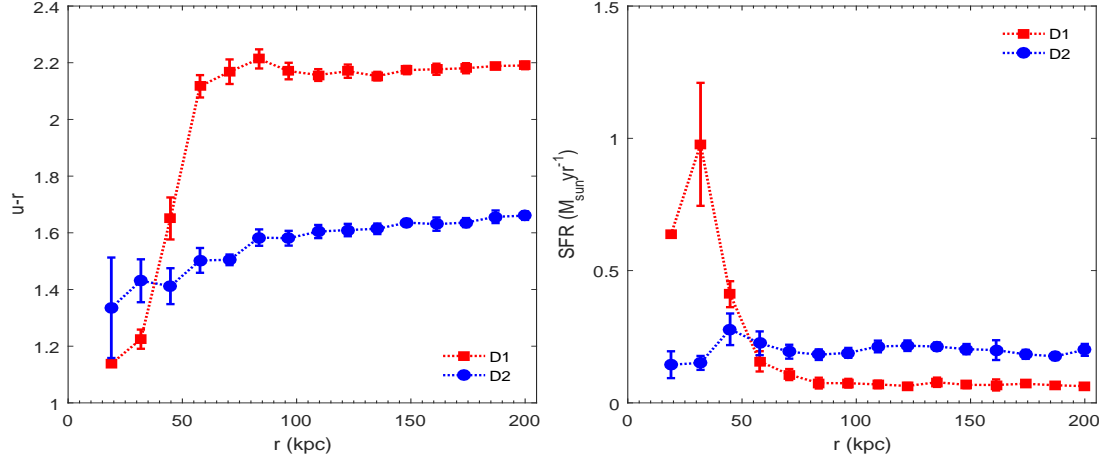


Fig. 5: Same as Figure 1 but after discarding the major pairs for which the 5<sup>th</sup> nearest neighbour lies within a distance of 500 kpc to 1 Mpc.

Major pairs	$D_{KS}$		$D_{KS}(\alpha)$				
	$\log(M_{\text{stellar}}/M_{\text{sun}})$	$Mass_{\text{coldgas}}(10^9 M_{\text{sun}})$	99%	90%	80%	70%	60%
All	0.1037	0.5105	0.1292	0.0972	0.0852	0.0773	0.0712
$r < 50$ kpc	0.1032	0.3512	0.3754	0.2826	0.2478	0.2249	0.2072
$r \geq 50$ kpc	0.1055	0.5104	0.1388	0.1043	0.0915	0.0830	0.0765

Table 2: This table shows the summary of the Kolmogorov-Smirnov (KS) tests carried out for a comparison of  $\log(M_{\text{stellar}}/M_{\text{sun}})$  and  $Mass_{\text{coldgas}}$  of major pairs in filaments and sheets. Separate comparisons are also carried out for major pairs having  $r < 50$  kpc and  $r \geq 50$  kpc. The table lists the KS statistic  $D_{KS}$  along with the critical values  $D_{KS}(\alpha)$  beyond which the null hypothesis can be rejected at a given confidence level.

Major pairs	$D_{KS}$		$D_{KS}(\alpha)$				
	$\log(M_{\text{halo}}/M_{\text{sun}})$		99%	90%	80%	70%	60%
	0.6532		0.1292	0.0972	0.0852	0.0773	0.0712

Table 3: This table shows Kolmogorov-Smirnov statistic  $D_{KS}$  for comparison of  $\log(M_{\text{halo}}/M_{\text{sun}})$  of major pairs residing in D1 and D2 type environments. It also shows the critical values  $D_{KS}(\alpha)$  above which the null hypothesis can be rejected at different confidence level.

The stellar mass (Birnboim & Dekel 2003; Dekel & Birnboim 2006; Bamford, Nichol & Baldry 2009) and the available cold gas mass content (Saintonge et al. 2012; Violino et al. 2018; Thorp et al. 2022) also play a very important role in deciding the star formation rate in galaxies. We test if the differences occurring in  $u - r$  colour and SFR of galaxies in major pairs residing in D1 and D2 type environments arise due to the differences in their stellar mass and cold gas content. We use a KS test to compare the distributions of stellar mass and cold gas mass of major paired galaxies in D1 and D2 type environments. The probability distribution functions of the two properties in D1 and D2 type environments are shown in the two panels of Figure 2. We first carry out the test for the major pairs with all possible pair separations. We then conduct separate tests for the major pairs with pair separation  $> 50$  kpc and  $< 50$  kpc. The results for the KS test are tabulated in Table 2. We note that null hypothesis for all the major pairs can be rejected at 90% and 99% confidence levels for stellar mass and cold gas mass respectively. This implies that the stellar mass distribution of galaxies in major pairs residing in D1 and D2 type environment are likely to be drawn from the same parent population. However, the galaxies in major pairs from filaments and sheets have a significantly different cold gas mass distribution. We

also arrive at the same conclusions for the major pairs with  $r > 50$  kpc. Interestingly, the results for the major pairs with  $r < 50$  kpc suggest that the null hypothesis for stellar mass can be rejected at a very low confidence level ( $< 60\%$ ), whereas for cold gas mass, it can be rejected at  $\leq 90\%$  confidence level. Thus, stellar mass of major pair galaxies with  $r < 50$  kpc in *D1* and *D2* type environment are highly likely to be drawn from the same underlying population. This clearly shows that stellar mass and available cold gas mass of the paired galaxies are not responsible for the differences observed in their  $u - r$  colour and SFR in *D1* and *D2* type environments at smaller pair separations ( $r < 50$  kpc).

Each galaxy is believed to have formed within a dark matter halo. The properties of the galaxy are expected to be intimately connected to the mass of the dark matter halo. In fact, the mass of the dark matter halo is believed to be the most important parameter that determines the properties of a galaxy (Cooray & Sheth 2002). The amount of substructures in the dark matter halos increases with the increasing halo mass (Gao et al. 2004; Pandey et al. 2013). There are observational evidences in favour of the correlations between substructure and star formation fraction in galaxy clusters (Bravo-Alfaro et al. 2009; Cohen et al. 2014). Substructures can also influence the stellar population in the galaxy (Helmi 2020). We show the distributions of the halo masses in the paired galaxies in filaments and sheets in Figure 3. The halo masses are obtained within the same aperture as the galaxies. We perform a KS test to find that the halo mass distribution of the paired galaxies in sheets and filaments are significantly different (Table 3). We find that the halo mass of the paired galaxies in sheets are relatively more massive than those residing in the filaments. The effects of the halo mass may also come from the virial shock heating of the halo gas that becomes important at masses greater than  $10^{12} M_{sun}$  (Birnboim & Dekel 2003). Such heating can suppress the supply of cold gas by preventing cold streams from the intergalactic medium. However, we find that none of the paired galaxies in filaments and sheets in our sample resides in such massive dark matter halo. At low masses, the supernova feedback may expel or heat the gas reservoir and quench the star formation (Kaviraj et al. 2007). The halo mass may have a role in shaping the physical properties of the galaxy pairs in filaments and sheets. But it is difficult to explain the cross-overs observed in Figure 3 using these differences in the halo mass distributions.

The filaments appear at the intersection of sheets and are generally denser compared to the sheets. Studies with N-body simulations suggest a successive flow of matter from voids to sheets, sheets to filaments and from filaments to clusters (Ramachandra & Shandarin 2015; Galárraga-Espinosa, Garaldi, & Kauffmann 2022). A number of earlier studies find that the galaxy pairs are preferentially aligned with the filament axis (Tempel & Tamm 2015; Mesa et al. 2018). The alignment signal is reported to be stronger for closer pairs residing near the filament spine. The anisotropic accretion along the filaments may significantly influence the gas accretion efficiency in these aligned galaxy pairs and trigger interaction induced star formation in them. Contrarily, the major pairs with  $r > 50$  kpc show a lower star formation in filaments than in sheets. The filaments are generally denser than the sheets. The *D1*-type galaxies are embedded in high density environment as compared to the *D2*-type galaxies (Pandey & Sarkar 2020). The galaxies in denser environments are known to be redder and low star forming (Lewis et al. 2002; Gómez et al. 2003; Kauffmann et al. 2004). So naively one would expect the galaxies in filamentary environment to be less star forming and redder compared to the galaxies in sheet-like environment. We find that this is true for the galaxies in major pairs with separation larger than 50 kpc. However, the galaxies in major pairs at closer pair separation show a strikingly opposite behaviour.

We do not analyze the alignment of the galaxy pairs in our study. The individual sheets and filaments can not be identified using the local dimension. We plan to carry out a detailed study of the galaxy pair alignment with different identification techniques of the cosmic web in a future work.

The Eagle simulation provides two definitions for the position of galaxies. These are based on the centre of mass and the location of the minimum of the gravitational potential. The two positions do not coincide for some galaxies. In this work, we use the centre of mass to define the position of galaxies. We also repeat our analysis considering the minimum of the gravitational potential as the position of a galaxy. We show the results of this analysis in Figure 4. The main findings of our analysis remain unchanged with this alternative definition of galaxy position. Further, it is important to ensure that the major pairs considered in our analysis do not belong to the galaxy groups. We measure the distances to



the 5<sup>th</sup> nearest neighbours for the paired galaxies in sheets and filaments and find that  $\sim 20\%$  of them have their 5<sup>th</sup> nearest neighbour within a distance of 500 kpc to 1 Mpc. We discard these galaxy pairs and repeat our analysis. The results of this analysis are shown in Figure 5. We find that discarding such galaxy pairs do not alter our results.

The results reported in this work are very similar to the results obtained in a recent study (Das, Pandey & Sarkar 2023) of the colour and SFR of major pairs in filaments and sheets using the SDSS data. Das, Pandey & Sarkar (2023) use volume limited sample of galaxies ( $M_r \leq -19$ ) for their analysis and find a crossover in these properties at nearly the same length scale ( $\sim 50$  kpc). It is interesting to note that we observe exactly the same trend in the EAGLE simulation data. This provides a strong theoretical support to the observational findings that large-scale structures like sheets and filaments affect galaxy interactions. This also indicates that the galaxy properties are modulated by the geometry of their large-scale environment.

Finally, we conclude that the filaments play a significant role in deciding the colour and star formation rate in galaxies. The observed differences in the colour and SFR of major pairs in filaments and sheets can not be interpreted in terms of the differences in the local density and the stellar mass distributions. The interacting galaxy pairs with smaller pair separation can trigger star formation. The filaments provide a favourable environment for such interactions. This makes the interacting galaxies bluer in filaments compared to those found in sheets.

**Acknowledgements** BP acknowledges financial support from the SERB, DST, Government of India through the project CRG/2019/001110 and support from IUCAA, Pune through the associateship programme. SS acknowledges DST, Government of India for support through a National Post Doctoral Fellowship (N-PDF).

The authors acknowledge the Virgo Consortium for making their simulation data publicly available. The EAGLE simulations were performed using the DiRAC-2 facility at Durham, managed by the ICC, and the PRACE facility Curie based in France at TGCC, CEA, Bruyères-le-Châtel.

## References

- Alonso, M. S., Tissera, P. B., Coldwell, G., Lambas, D. G., 2004, MNRAS, 352, 1081 3
- Baldry, I. K., Glazebrook, K., Brinkmann, J., Ivezić, Ž., Lupton, R. H., Nichol, R. C. & Szalay, A. S., ApJ, 600, 681 6
- Balogh, M. L., Navarro, J. F., & Morris, S. L., 2000, ApJ, 540, 113 2
- Bamford, S. P., Nichol, R. C., Baldry, I. K., et al., 2009, MNRAS, 393, 1324 7
- Barton, E. J., Geller, M. J., Kenyon, S. J., 2000, ApJ, 530, 660 2
- Bhattacharjee, S., Pandey, B., & Sarkar, S., 2020, JCAP, 2020, 039 2
- Birnboim Y., Dekel A., 2003, MNRAS, 345, 349 2, 7, 8
- Bond, J. R., Kofman, L., & Pogosyan, D., 1996, Nature, 380, 603 2
- Bravo-Alfaro H., Caretta C. A., Lobo C., Durret F., Scott T., 2009, A&A, 495, 379 8
- Cohen S. A., Hickox R. C., Wegner G. A., Einasto M., Vennik J., 2014, ApJ, 783, 136 8
- Cox, T. J., Primack, J., Jonsson, P., & Somerville, R. S., 2004, ApJL, 607, L87 2
- Corray, A., Sheth, R.K., 2002, Phys. Rep., 371, 1 8
- Das, A., Pandey, B & Sarkar, S., 2023, RAA, 02, 23 1, 2, 3, 9
- Galarraga-Espinosa, D., Aghanim, N., Langer, M., Tanimura, H., 2021, A&A, 649, A117 2
- Galarraga-Espinosa D., Garaldi E., Kauffmann G., 2022, arXiv, arXiv:2209.05495, Accepted in A&A 8
- Davé R., Finlator K., Oppenheimer B. D., 2012, MNRAS, 421, 98 3
- Davis, M., & Geller, M.J., 1976, ApJ, 208, 13 2
- Dekel A., Birnboim Y., 2006, MNRAS, 368, 2 2, 7
- Dekel, A., Sari, R., Coverino, D., 2009, ApJ, 703, 785 3
- Doi, M et al., 2010, doi:10.1088/004-6256/139/4/1628, arxiv:1002.3701 3
- Dressler, A., 1980, ApJ, 236, 351 2
- Einasto J., Joeveer M., Saar E., 1980, MNRAS, 193, 353 2

- Ellison, S. L., Patton, D. R., Simard, L., McConnachie, A. W., Baldry, I. K., Mendel, J. T., 2010, MNRAS, 407, 1514 2
- Gabor J. M., Davé R., Finlator K., Oppenheimer B. D., 2010, MNRAS, 407, 749
- Gao L., White S. D. M., Jenkins A., Stoehr F., Springel V., 2004, MNRAS, 355, 819. doi:10.1111/j.1365-2966.2004.08360.x 8
- Gómez, P. L., Nichol, R. C., Miller, C. J., Balogh, M. L., Goto, T., Zabludoff, A. I., Romer, A. K., et al., 2003, ApJ, 584, 210 2, 8
- Goto, T., Yamauchi, C., Fujita, Y., Okamura, S., Seikiguchi, M., Smail, I., Bernardi, M., & Gomez, P.L., 2003, MNRAS, 346, 601 2
- Gregory S. A., Thompson L. A., 1978, ApJ, 222, 784 2
- Gunn, J. E., & Gott, J. R., 1972, ApJ, 176, 1 2
- Guzzo, L., Strauss, M.A., Fisher, K.B., Giovanelli, R., & Haynes, M.P., 1997, ApJ, 489, 37 2
- Helmi A., 2020, ARA&A, 58, 205 8
- Joeveer M., Einasto J., 1978, IAUS, 79, 241 2
- Kaviraj S., Kirkby L. A., Silk J., Sarzi M., 2007, MNRAS, 382, 960 8
- Kauffmann, G., White, S. D. M., Heckman, T. M., et al., 2004, MNRAS, 353, 713 2, 8
- Kauffmann, G., Heckmann, T. M., White, S. D. M., Charlot, S., Tremonti, C et al., 2003, MNRAS, 341, 54 4
- Larson, R. B., Tinsley, B. M., & Caldwell, C. N., 1980, ApJ, 237, 692 2
- Lewis, I., Balogh, M., Propris, R. De., Couch, W., Bower, R., Offer, A., Bland-Hawthorn, J., et al., 2002, MNRAS, 334, 673 2, 8
- Martig M., Bournaud F., Teyssier R., Dekel A., 2009, ApJ, 707, 250 2
- Masters K. L., Mosleh M., Romer A. K., Nichol R. C., Bamford S. P., Schawinski K., Lintott C. J., et al., 2010, MNRAS, 405, 783 2
- McAlpine, S., Helly, J. C., Schaller, M., Trayford, J. W. et al., 2016, A&C, 72, 15 3
- Mesa V., Duplancic F., Alonso S., Muñoz Jofré M. R., Coldwell G., Lambas D. G., 2018, A&A, 619, A24 2, 8
- Moore, B., Katz, N., Lake, G., Dressler, A., & Oemler, A., 1996, Nature, 379, 613 2
- Moore, B., Lake, G., & Katz, N., 1998, ApJ, 495, 139 2
- Murray, N., Quataert, E., & Thompson, T. A., 2005, ApJ, 618, 569 2
- Nikolic, B., Cullen, H., Alexander, P., 2004, MNRAS, 355, 874 2
- Oemler, A., 1974, ApJ, 194, 1 2
- Pandey, B., & Bharadwaj S., 2005, MNRAS, 357, 1068 2
- Pandey, B., & Bharadwaj, S., 2006, MNRAS, 372, 827 2
- Pandey, B., & Bharadwaj, S., 2008, MNRAS, 387, 767 2
- Pandey B., White S. D. M., Springel V., Angulo R. E., 2013, MNRAS, 435, 2968 8
- Pandey, B., & Sarkar, S., 2017, MNRAS, 467, L6 2
- Pandey, B., & Sarkar, S., 2020, MNRAS, 498, 6069 2, 8
- Park, C., et al. 2005, ApJ, 633, 11 2
- Patton, D. R., Ellison, S. L., Simard, L., McConnachie, A. W., Mendel, J. T., 2011, MNRAS, 412, 591 2
- Peng Y.-jie., Renzini A., 2020, MNRAS, 491, L51 2
- Planck Collaboration et al., 2014, A&A, 571, A1 3
- Ramachandra N. S., Shandarin S. F., 2015, MNRAS, 452, 1643 8
- Saintonge A., Tacconi L. J., Fabello S., Wang J., Catinella B., Genzel R., Graciá-Carpio J., et al., 2012, ApJ, 758, 73 7
- Sarkar, P. & Bharadwaj, S., 2009, MNRAS, 394, L66 3, 4
- Sarkar, S., & Pandey, B., 2019, MNRAS, 485, 4743 4
- Sarkar, S., & Pandey, B., 2020, MNRAS, 497, 4077 2
- Silk, J., 1977 ApJ, 211, 638 2
- Somerville, R. S., & Primack, J. R., 1999, MNRAS, 310, 1087 2
- Springel, V., Di Matteo, T., & Hernquist, L., 2005, MNRAS, 361, 776 2

- Tempel E., Tamm A., 2015, *A&A*, 576, L5 2, 8
- Thorp M. D., Ellison S. L., Pan H.-A., Lin L., Patton D. R., Bluck A. F. L., Walters D., et al., 2022, *MNRAS*, 516, 1462 7
- Trayford, J. W et al., 2015, *MNRAS*, 452, 2879 3
- Tuominen T., Nevalainen J., Tempel E., Kuutma T., Wijers N., Schaye J., Heinämäki P., et al., 2021, *A&A*, 646, A156 2
- Violino G., Ellison S. L., Sargent M., Coppin K. E. K., Scudder J. M., Mendel T. J., Saintonge A., 2018, *MNRAS*, 476, 2591 7
- White, S. D. M., & Rees, M. J., 1978 *MNRAS*, 183, 341 2
- Woods, D. F., Geller, M. J., 2007, *AJ*, 134, 527 2
- Zehavi, I., et al. 2005, *ApJ*, 630, 1 2
- Zeldovich I. B., Shandarin S. F., 1982, *PAZh*, 8, 131 2